Proc. of the International Conference on Electrical, Computer, Communications and Mechatronics Engineering (ICECCME 2023)
19-20 July 2023, Tenerife, Canary Islands, Spain

Potential detection of Flavescence dorée in the vineyard using close-range hyperspectral imaging

Marko Barjaktarovic
School of Electrical Engineering, University of Belgrade, Serbia
Remote Sensing Laboratory, University of Trento, Italy
mbarjaktarovic@etf.bg.ac.rs

Massimo Santoni
Remote Sensing Laboratory, Department of Information Engineering and Computer Science
University of Trento, Italy
massimo.santoni@unitn.it

Michele Faralli
Center Agriculture Food Environment (C3A), University of Trento, Italy
Research and Innovation Centre, Fondazione Edmund Mach, Italy
michele.faralli@unitn.it

Massimo Bertamini
Center Agriculture Food Environment (C3A) University of Trento, Italy
Research and Innovation Centre, Fondazione Edmund Mach, Italy
massimo.bertamini@unitn.it

Lorenzo Bruzzone
Remote Sensing Laboratory, Department of Information Engineering and Computer Science
University of Trento, Italy
lorenzo.bruzzone@unitn.it

***Abstract*—Grapevine is one of the most important crops cultivated across Europe. Climate factors and diseases constantly threaten its production. Recently, Flavescence dorée (FD), an incurable grapevine disease with the obligation to uproot each infected plant, has been widely spread in Europe. The symptoms of FD are visually expressed in the late summer. Currently, the adopted procedure consists in scouting for infected plants by trained experts, which is time-consuming and not frequent enough. As stress development causes subtle spectral changes before any visible symptoms appear, during the summer of 2022, hyperspectral and multispectral images were acquired in the two vineyards near Riva del Garda, Trentino, Italy. A classification accuracy between 90.2 % and 96.9 % in distinguishing between infected and healthy plants was obtained from the hyperspectral data. These findings justify further efforts to use an in-house developed, affordable multispectral camera, significantly reducing equipment cost and procedure complexity while mapping the relevant spectral channels.**

Keywords—Grapevine disease detection, Flavescence dorée, Hyperspectral imaging, Multispectral camera, Remote sensing.

I. INTRODUCTION

For Europe, the grapevine is not only highly important as the world's third most valuable horticultural crop [1] but, due to its high socioeconomic role, it embodies a tangible cultural heritage, demonstrated by the diversity of grapevine cultivars and viticultural practices [2]. The economic impact for Europe reflects 3.2 million hectares or 45 % of the world's total wine-growing areas, where Spain, France, and Italy together accounted for three-quarters (74.9 %) of it [3]. Due to climate change, grapevine production is under constant threat, especially with drought and heat waves during spring and summer, when prolonged exposure to extremely high temperatures can negatively affect the plant's photosynthetic system. Water deficit is one of the leading environmental factors limiting vegetative growth and berry quality, increasing grape malic acid concentration [4]. An additional hazard on grapevine yield is put by grapevine trunk diseases [2], among which Flavescence dorée (FD) introduces severe consequences and can reduce production between 51 % and 92 % compared to healthy plants [5].

Flavescence dorée is an incurable, severe epidemic disease of grapevine in Europe caused by FD-phytoplasma. It is transmitted from one plant to another with grafting or by the leafhopper Scaphoideus titanus Ball [6]. FD is considered one of the most important diseases for the European principal wine-production areas. Therefore, it is a quarantine disease with the following mandatory control procedures: use of healthy plant material, spraying insecticides against the vector, and uprooting each infected plant to eliminate sources of FD phytoplasma [7]. An additional obligation is to remove the whole vineyard when the infection exceeds 20 % of all plants. Entire vineyard uprooting is causing significant financial damage in the current year and for the next 3-5 years since new grapevines need time to guarantee a substantial yield. As compensation for losses due to the FD, only in 2005, Italian grapevine growers were supported with 34 million euros [5].

Furthermore, the FD is constantly spreading. For example, in Piedmont (Italy), from 2003 to 2018, FD increased from a very restricted zone to almost 25 % of the whole Piedmont grapevine area [8]. In Trentino Alto-Adige (Italy), FD's presence nearly doubled in just one year (from 2021 to 2022) [9]. Therefore, to prevent the spreading of FD not only in a

The findings presented in this paper are results from "MCAPEFA" projects. This project has received funding from the European Union's Horizon 2020 research and innovation programme under the Marie Sklodowska-Curie grant agreement No 101028085.

monitored vineyard but also to neighboring ones, it is essential to detect even a single infected plant over an entire area [10].

FD's primary visible symptoms manifest during the summer. These symptoms are characterized by leaves rolling downwards and acquiring a reddish or yellowish hue in red and white cultivars, respectively (Fig. 1). Additionally, shoots exhibit a lack of lignification, while berries display signs of wilting and drying out [5]. The symptoms progressively spread within the canopy during the vegetative season [8]. The visible signs usually appear at least a year after infection, but not necessarily every year and not on all the branches [11]. Currently, the only available solution is to scout vineyards for infected plants. It is conducted by trained agronomists and experts. However, this is a time-consuming task, and usually, each vineyard is controlled once in one or two years due to a lack of skilled individuals, leaving too much time for FD to spread around [[5], [12]]. Hence, there is high demand for an automatic tool capable of detecting FD symptoms and localizing infected zones. It will allow localized and direct treatment of contaminated vines, reducing soil and water pollution compared with the current procedure, which requires up to 10 spraying treatments yearly in the whole field [13].

Fig. 1. FD symptoms in red (left - Cabernet Sauvignon) and white (right - Chardonnay) grapevine variety.

Evidence shows that FD influences photosynthetic capacity alongside other morphological changes, such as leaf rolling. It is especially valid for hyperspectral data, where the progression of stress development causes subtle spectral changes before any visible symptoms appear [14]. Several attempts to detect FD using hyperspectral or multispectral cameras have been found in remote sensing literature.

In [[10], [15]], researchers used a standard multispectral camera (5 bands) to detect FD. The results indicated that FD and GTD (Grapevine Trunk Disease, another grapevine with similar symptoms) could be detected, with a misclassification between these two diseases and the success rate depending on the grape variety (red or white grapes). It was suggested that misclassifications could be related to the presence of mixed soil/vine vegetation or shadow/vine vegetation pixels. Segmentation can be improved with higher ground spatial resolution. Bendel et al. [16] investigated the possibility of FD detection using hyperspectral data in laboratory conditions with uniform illumination and the same imaging geometry. Although a high correct classification rate was obtained (accuracy was 96 % or more depending on variety), further research is needed to identify optimal bands for application in vineyards. With a similar hyperspectral acquisition setup, an accuracy of 83 % was achieved with a deep learning approach [17]. However, additional work is required to adapt the process for in-field testing and reduce the data dimensionality. Promising detection results (precision: 0.92 and 0.89, recall: 0.76 and 0.75 for two grapevine varieties) were obtained by using the object detection algorithm YOLOv4-tiny and RGB images taken in the vineyard [5]. Still, all infected samples have highly expressed symptoms. Al-Saddik et al. acquired hyperspectral data in the field with a handheld device, collecting four profiles per leaf within a range from 350 nm to 2500 nm. The author's first conclusion was that there is no unique optimal index for recognizing FD in all scenarios [18]. The most suitable index relies upon the grapevine species, soil, vegetation, and climate conditions. Authors ascertained that creating indices based on the spectral diversities resulting from FD is viable, but this should be tuned on the precise context [18]. They continued research by selecting eight optimal bands for different scenarios in the whole acquired wavelength range [19]. Their next step was to choose seven wavelengths up to 1000 nm [12]. A multispectral system can be implemented in this range with Silicon as the low-cost sensing material. Their most recent work presents a protocol for constructing a multispectral system that consists of 4 standard cameras, each with a different narrowband filter [13]. The number of filters was reduced to four due to dimension and weight constraints, as the authors planned that the final device should be mounted on a low-altitude UAV. To compensate for the reduction of spectral data to only four reflectance values, the authors added 4 Haralick texture features for each channel to improve classification accuracy. The resulting accuracy was between 80.7 % and 92.8 %, depending on grapevine varieties. The authors suggested that additional work is needed for geometric and radiometric correction to address shadowing and reflectance from other surrounding objects. Further, they proposed that some other pattern recognition methods can be integrated into the procedure with spatial variability of data. Interesting conclusions come from [20], where findings were based on spatial change of three spectral indices (NDVI, NDRE, and VIS/NIR ratio) in each monitored grapevine row. Data were acquired using an active optical sensor which measured point reflectance at three different wavelengths (670 nm, 730 nm, and 775 nm) directly in the vineyard, with an approximate distance of 80 cm from the plant and 50 cm between each measurement. The authors showed a strong correlation between FD's occurrence and spatial change of the three selected indices.

This paper presents research with a similar approach to the protocol described by Al-Saddik et al. [13]. However, instead of acquiring hyperspectral data at each leaf in a highly controlled procedure, this work uses a hyperspectral camera in the same position as an in-house developed multispectral device. The plan is to use the multispectral camera as a final device for scouting the FD presence. This setup investigated the possibility of FD detection using spectral profiles obtained in the scenario where the influence of leaf orientation, distance from the camera, shadowing, and multi-scattering effect occur. As spectral profiles for leaves with highly expressed symptoms have noticeable differences compared to the green leaves, the testing was restricted to green leaves for both infected and healthy plants. This way assesses the possibility of detecting FD when

the discoloration of leaves is not highly expressed, which can lead to its earlier detection. First, this research tested if this detection is feasible when the symptoms are visually noticeable on the data acquired in September 2022. The results show classification accuracy of 96.1 % for Cabernet Sauvignon and 96.9 % for Chardonnay. Next, the possibility of performing the detection is checked on the data acquired in July 2022, when symptoms have a lower severity level. The classification accuracies of 91.5 % for Cabernet Sauvignon and 90.6 % for Chardonnay were achieved. This is still quite accurate and justifies the intention to try the designed multispectral device to search for FD presence.

Fig.2. presents green leaves for both Cabernet Sauvignon and Chardonnay when there are no FD symptoms (a and b), with signs in July (c and d) and in September (e and f). It is difficult to spot differences between images of healthy and infected leaves, even in September. Indeed, there are some changes in the leave's texture, but a lot of experience and training are needed to notice them in the early stage. On the contrary, those differences can be detected in hyperspectral data as they influence reflected spectra.

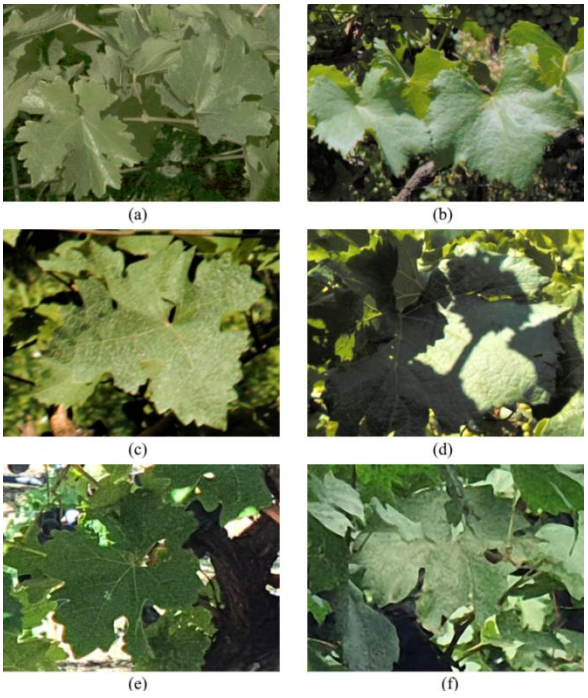

Fig. 2. Example of healthy and infected green leaves. Cabernet Sauvignon: (a) healthy, (c) infected from July, (e) infected from September. Chardonnay: (b) healthy, (d) infected from July, (f) infected from September.

The following section describes the acquisition setup, with a selection of spectral profiles and their pre-processing. Section III explains classification and presents the obtained result. Finally, the conclusion and suggestions for future work are given in Section IV.

II. Acquisition and Pre-processing of Hyperspectral Data

Data were acquired on two vineyards close to Riva del Garda. One is with Cabernet Sauvignon (location Bolognano) as representative of the red grapevine variety, while the second is with the white grape variety Chardonnay (location Nago-Torbole). For these two vineyards, some plants with FD were discovered in 2021 (due to the mandatory procedure, they were uprooted). Thus it was likely that FD would be found on the date of acquisition, as both varieties are highly susceptible to FD (Cabernet Sauvignon shows the highest vulnerability) [21].

Campaigns were conducted on 12th July and 22nd September 2022, between 10:00 and 13:00 in Bolognano and 14:30 and 17:30 in Nago-Torbole. On both days, it was sunny weather with occasionally a few clouds resulting in an illumination variation that better represents different acquisition conditions. Obtained hyperspectral data contains images of 5(8) healthy and 4(6) infected plants in Bolognano, while in Nago-Torbole, 7(8) healthy and 6(7) infected plants in July (September) were imagined.

For both campaigns, an FD presence in each plant was assessed in the field by a local expert who regularly visually observes vineyards to spot newly infected plants and prevent further spreading.

Fig. 3 shows equipment for data acquisition. It consists of hyperspectral scanner HySpex Mjolnir V-1240, with 200 channels in the 400 – 1000 nm range and 1240 samples in each channel. The images are obtained by moving the pushbroom scanner by a slider. The in-house assembled imaging device includes the designed multispectral camera and a thermal camera (Seek Mosaic Thermal Core, with a resolution of 320x240 pixels). This device was mounted on a standard photographic tripod, together with the high-quality thermal camera FLIR Duo Pro R as a temperature reference sensor.

Fig. 3. Equipment used during both campaigns.

The multispectral camera was built using Raspberry Pi 4 and Arducam Quad-Camera Bundle Kit (four 1 MPx OmniVision OV9782 global shutter sensors), with one single, one dual, and two triple band filters obtaining nine different narrow bands with following central wavelengths 432, 517, 550, 577, 615, 660, 690, 750, 850 nm. The radiance in each band was reconstructed using the procedure described in [22], [23]]. Previously, calibration was performed in the laboratory using the same hyperspectral scanner, X-Rite® ColorChecker Classic, with 24 uniform patches as the target and QTH (Quartz Tungsten Halogen) as a light source. A thermal sensor was included since a detectable thermal difference between healthy and infected plants was reported [24]. In the future, improving the detection of FD using multispectral images with thermal data will be considered. The developed multispectral device is shown in Fig. 4. Cameras in

the visible and near-infrared bands are grouped in the right part of the housing, while the thermal camera is toward the left part (considering the orientation of Fig. 4).

Fig. 4. Designed imaging device with multispectral and thermal cameras.

The main reasons for the future use of multispectral and thermal cameras are drastically reducing needed investment and the amount of generated data that must be processed. Information from several spectral bands and thermal data is likely enough to distinguish between infected and healthy plants with satisfying accuracy. In that case, it will both reduce the cost of equipment, and it will simplify the complexity of the procedure.

In each hyperspectral image acquired in July and September, a number of rectangular regions of interest (ROI), varying between 20 and 40, were selected (see Fig. 5). Each ROI was extracted as a patch from one green leaf. The complete patch was exposed to sunlight or was in the shadow. After calculating the average profile in each ROI, the average value was divided by the average spectral radiance of the white box to get reflectance. Spectral radiances of the white box in shadow and in the sunlight were acquired several times while collecting data in each vineyard. Using the described procedure, 110 (112) and 131 (134) reflectance profiles of healthy and infected plants were prepared, respectively, in July (September), for Cabernet Sauvignon and 104 (120), and 106 (121) for Chardonnay.

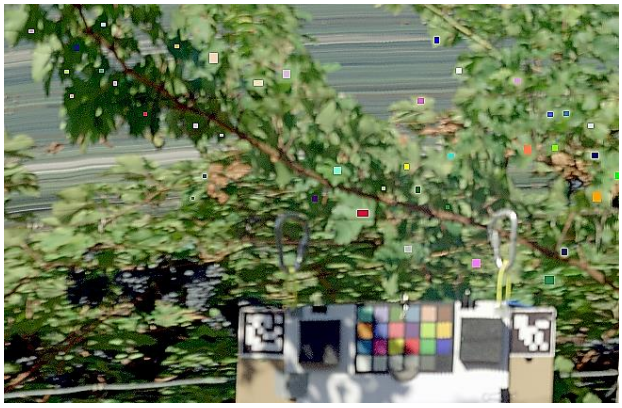

Fig. 5. Example of rectangle ROI used for obtaining reflectance profiles in one of the hyperspectral images of an infected plant.

Several optical phenomena must be considered when applying close-range hyperspectral sensing for plant monitoring in natural conditions. The radiance of an observed leaf can include additive polynomial terms R^2, RT, T^2, R^3, ..., where R and T are, respectively, the reflectance and transmittance of the surrounding leaves [25]. Then, the radiance sensed by the detector is highly affected by the inclination of the leaf toward the illumination and by the distance between the leaf and the sensor [14].

There are two common methods, the Multiplicative Scatter Correction (MSC) and Standard Normalize Variate (SNV) [14, [25]], suitable to compensate for the described phenomena. SNV does not require a predefined reference spectrum, thus it was used for pre-processing spectral data. With SNV, each profile is divided by its standard variance after subtracting its mean value. This normalization removes huge differences in reflectivity, especially in the near-infrared portion of the spectrum, where high reflectance from the leaves occurs. Due to multi-scattering phenomena, several reflections add together, resulting in high variation in the spectrum. This should be removed to properly classify the data. Fig. 6 shows the effect of SNV correction.

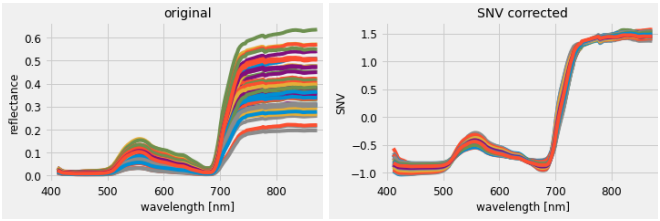

Fig. 6. Example of reflectance spectra before and after SNV correction for a healthy plant of Chardonnay variety.

III. Classification Results

The feature vector for classifying one spectral profile as healthy (class 0) or infected (class 1) contains all wavelengths up to 880 nm, i.e., 160 reflectance values. Higher wavelengths were excluded as a high noise level is present in that part of the spectrum [14]. Wavelength 880 nm was selected as the upper end of the passband for the last narrowband filter in the designed multispectral camera, centered at 850 nm. A Multi-Layer Perceptron (MLP) neural network was chosen as the binary classifier, as MLP is frequently used to model complex relationships between inputs and outputs in the scientific literature [13]. In this study, one hidden layer with ten neurons is placed between the input and output layers. To prevent overfitting of the model on training data and to better predict unseen data, *k*-fold cross-validation was used [26], where *k* was set to 10, splits were dataset-wise, and $n = 5$ repeats were conducted to reduce the error in the estimate of the mean model performance. All code was implanted in Python programming language.

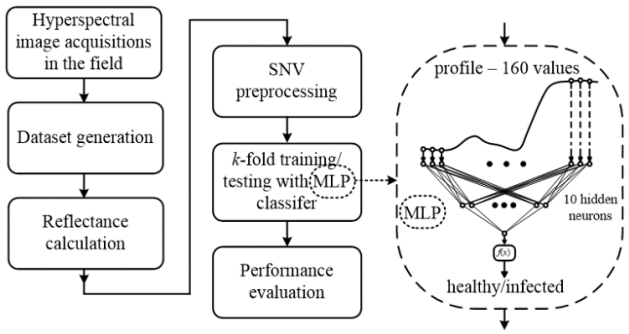

Fig. 7. Flowchart with all steps of conducted research, from image acquisition to classification.

Fig. 7 presents the flowchart of the adopted methodology together with the structure of the MLP classifier.

Table 1. shows mean values and standard deviation for accuracy, precision, and recall. With the data acquired in September, the mean classification accuracy for both varieties is very high, i.e., 96.1 % and 96.9 % for Cabernet Sauvignon and Chardonnay, respectively. The higher value for the Chardonnay variety may be explained by the fact that the texture of the Chardonnay's leaf is rougher compared with Cabernet Sauvignon. This texture might induce more differences in reflectance spectra when symptoms are expressed. An additional test using all data together resulted in lower mean accuracy than for separate tests of each variety. These findings align with the other authors' conclusion that each grapevine variety requires fine-tuning of the classification algorithm.

TABLE I. CLASSIFICATION RESULTS

Month	***Grapevine variety***	***Accuracy [%] mean (std)***	***Precision [%] mean (std)***	***Recall [%] mean (std)***
Sept.	CS	96.1 (3.2)	97.4 (3.9)	95.4 (5.5)
	Ch	96.9 (3.9)	97.7 (5.1)	96.1 (6.4)
	CS and Ch	92.3 (4.2)	93.3 (4.4)	92.0 (7.0)
July	CS	91.5 (5.2)	91.3 (6.3)	93.9 (7.4)
	Ch	90.2 (3.5)	89.2 (5.1)	91.7 (4.8)
	CS and Ch	88.3 (2.5)	88.3 (2.5)	89.2 (4.0)

CS - Cabernet Sauvignon, Ch - Chardonnay, std - standard deviation

The results were different when using data collected in July. The mean accuracies are smaller than in September but still very satisfactory, i.e., 91.5 % and 90.2 % for Cabernet Sauvignon and Chardonnay, respectively. In this one, Cabernet Sauvignon shows a slightly higher value than Chardonnay. That can be because Cabernet Sauvignon is the most susceptible grapevine variety to FD [21], and symptoms are expressed more rapidly in the first part of the season. As expected, lower mean accuracy was obtained with profiles for both varieties together.

Acquired data from July and September showed that the initial hypothesis is valid. Although visible symptoms are not easy to spot, the progression of FD develops subtle spectral changes that can be detected using a hyperspectral camera.

IV. Conclusion

This paper shows that FD detection can be accomplished by a hyperspectral camera using reflectance profiles for only green leaves when the discoloring is not highly expressed yet. The contribution of this research is not only in obtaining high accuracy but also in the proposed acquisition setup. As mentioned, previous researches were based on hyperspectral data collected in highly controlled conditions, which are unsuitable for in-field circumstances. For implementation in the field, acquired data must include variability influenced by multi-scattering, leaf orientation, the distance between leaves and the camera, and changes in incident light. Otherwise, when applied to the field, the trained detector could lead to the wrong classification. In this research, data were collected in conditions that represent actual vineyard scenarios. In this context, it was shown that hyperspectral pre-processing reduces enough variability in input data to provide high classification accuracy.

Furthermore, these results are the starting point for future work with the data acquired using the developed multispectral camera. The main goal is to reduce needed investment by several orders of magnitude. Despite the fact that high accuracy using a hyperspectral camera was obtained, its systematic use in the field is challenging due to the high price of this instrument. Also, in theory, it is possible to use this scanner on a vehicle. However, the main issue is the very high cost of that setup. The acquisition procedure is time-consuming, and during image collection, illumination conditions change which can influence accuracy. Time-varying illumination induces variation in the measured spectrum that can affect accuracy, which is considered a limitation of this research. Although taking images of the reference whiteboard to compensate for that effect was performed together with spectrum pre-processing technique, it would be appropriate to design and use a controlled illumination source, possibly placing a camera and illuminator inside a hood and on a cart or tractor to change position more rapidly in vineyards. This idea will be considered in future research.

As was stated, the exceptionally high price further restricts the application of hyperspectral scanners, and some solution based on more affordable multispectral cameras is needed. Planned future research is to test the possible FD detection using an in-house assembled multispectral system, which is in a lower price range compared to commercially available solutions with a similar number of bands. This device has nine bands thus, contains significantly less information than the channels of a hyperspectral camera. However, additional image features, such as texture-based, can improve classification results, and they will be considered in future research. Furthermore, some recent object detection algorithms, like those from the YOLO family, are alternative, promising methods for FD detection [5]. If the results are satisfying, a platform and procedure to verify this approach the next summer will be prepared.

As a final remark, images of only two grapevine varieties were acquired in the presented work. Although Cabernet Sauvignon and Chardonnay represent red and white grapes and are among the most cultivated grapevine varieties, it would be desirable to include other varieties to assess the generalization capabilities of the detector and provide a protocol for fine-tuning in each specific condition. This will be an additional direction for further improvement of current research.

Acknowledgment

The data collection for this research was done at two vineyards managed by the Agraria Riva del Garda (Italy). Thank to Agraria Riva del Garda company with its associates and Michele Mutinelli from Agraria, it was possible to collect and label the data.

References

[1] D. Cantu, M. A. Walker, The Grape Genome, Springer Nature Switzerland AG 2019.

[2] L. Guerin-Dubrana, F. Fontaine, and L. Mugnai, “Grapevine trunk disease in European and Mediterranean vineyards: occurrence, distribution and associated disease-affecting cultural factors”, *Phytopathol. Mediterr.*, vol. 58, no. 1, pp. 49-71, May 2019.

[3] Eurostat, Vineyards in the EU – statistics - May 2022, Available online: https://ec.europa.eu/eurostat/statistics-explained/index.php?title=Vineyards_in_the_EU_-_statistics (accessed on 15 March 2023)

[4] F. Droulia, and I. Charalampopoulos, "Future Climate Change Impacts on European Viticulture: A Review on Recent Scientific Advances," *Atmosphere*, vol. 12, no. 4, p. 495, April 2021.

[5] M. Tardif et al., "Two-stage automatic diagnosis of Flavescence Dorée based on proximal imaging and artificial intelligence: a multi-year and multi-variety experimental study," *OENO One*, vol. 56, no. 3, pp. 371–384, September 2022.

[6] M. Ripamonti et al., "Leafhopper feeding behaviour on three grapevine cultivars with different susceptibilities to Flavescence dorée," *J. Insect. Physiol.*, vol. 137, 104366, February–March 2022.

[7] J. Albetis et al., "On the Potentiality of UAV Multispectral Imagery to Detect Flavescence dorée and Grapevine Trunk Diseases," *Remote Sens.*, vol. 11, no. 1, p. 23, December 2018.

[8] M. Ripamonti et al., "Recovery from Grapevine Flavescence Dorée in Areas of High Infection Pressure," *Agronomy*, vol. 10, no. 10, p. 1479, September 2020.

[9] Il Dolomiti, "Flavescenza dorata, Manica: "Quasi raddoppiate in un anno le viti sintomatiche. Quale soluzione per frenare la diffusione in Trentino?"," Available online: https://www.ildolomiti.it/politica/2022/flavescenza-dorata-manica-quasi-raddoppiate-in-un-anno-le-viti-sintomatiche-quale-soluzione-per-frenare-la-diffusione-in-trentino (accessed on 10 March 2023)

[10] J. Albetis et al., "Detection of Flavescence dorée Grapevine Disease Using Unmanned Aerial Vehicle (UAV) Multispectral Imagery," *Remote Sens*., vol. 9, no. 4, p. 308, March 2017.

[11] A.S. Hania, J.C. Simon, and F. Cointault, "Development of Spectral Disease Indices for 'Flavescence Dorée' Grapevine Disease Identification," *Sensor*s, vol. 17, no. 12, p. 2772, November 2017.

[12] H. Al-Saddik, J.C. Simon, O. Brousse, F. Cointault, Multispectral band selection for imaging sensor design for vineyard disease detection: case of Flavescence Dorée, *Adv. Anim. Biosci.*, vol. 8, no. 2, pp. 150-155, 2017.

[13] H. Al-Saddik, A. Laybros, J.C. Simon, and F. Cointault, "Protocol for the Definition of a Multi-Spectral Sensor for Specific Foliar Disease Detection: Case of Flavescence Dorée". In: Musetti, R., Pagliari, L. (eds) Phytoplasmas. Methods in Molecular Biology, vol 1875. Humana Press, New York, 2019.

[14] M. S. M. Asaari et al., "Close-range hyperspectral image analysis for the early detection of stress responses in individual plants in a high-throughput phenotyping platform," *ISPRS J Photogramm.*, vol. 138, pp. 121-138, April 2018.

[15] J. Albetis et al., "On the Potentiality of UAV Multispectral Imagery to Detect Flavescence dorée and Grapevine Trunk Diseases," *Remote Sens*., vol. 11, no. 1, p. 23, December 2018.

[16] N. Bendel et al., "Detection of Two Different Grapevine Yellows in Vitis vinifera Using Hyperspectral Imaging," *Remote Sens.*, vol. 12, no. 24, p. 4151, December 2020.

[17] D. M.Silva et al., "Automatic detection of Flavescense Dorée grapevine disease in hyperspectral images using machine learning," *Procedia Comput. Sci.*, vol. 196, pp. 125-132, 2022.

[18] H. AL-Saddik, J.-C. Simon, and F. Cointault, "Development of Spectral Disease Indices for 'Flavescence Dorée' Grapevine Disease Identification," *Sensors*, vol. 17, no. 12, p. 2772, Nov. 2017.

[19] H. AL-Saddik, J.-C. Simon, and F. Cointault, "Assessment of the optimal spectral bands for designing a sensor for vineyard disease detection: the case of 'Flavescence dorée," *Precision Agric.*, vol. 20, pp. 398–422, 2019.

[20] G. Daglio et al, "Potential field detection of Flavescence dorée and Esca diseases using a ground sensing optical system," *Biosyst. Eng.*, vol. 215, pp. 203-214, March 2022.

[21] E. Sandrine et al, "Contrasting Susceptibilities to Flavescence Dorée in Vitis vinifera, Rootstocks and Wild Vitis Species," *Front. Plant Sci.*, vol. 7, November 2016.

[22] G. Themelis, J. S. Yoo, and V. Ntziachristos, "Multispectral imaging using multiple-bandpass filters," *Opt. Lett.*, vol. 33, no. 9, pp. 1023-1025, 2008.

[23] Y. Fawzy, S. Lam, and H. Zeng, "Rapid multispectral endoscopic imaging system for near real-time mapping of the mucosa blood supply in the lung," *Biomed. Opt. Express.*, vol 6. no. 8 pp. 2980-2990, August 2015.

[24] R. Ishimwe, K. Abutaleb, and F. Ahmed, "Applications of Thermal Imaging in Agriculture - A Review," *Adv. Remote Sen.*, vol. 3 no. 3, pp. 128-140, September 2014.

[25] N. Al Makdessi, M. Ecarnot, P. Roumet, and G. Rabatel, "A spectral correction method for multi-scattering effects in close range hyperspectral imagery of vegetation scenes: application to nitrogen content assessment in wheat," *Precision Agric.*, vol. 20, no. 2, pp. 237–259, Apr. 2019.

[26] S. Kathiravan, A. K. Cherukuri, D. R. Vincent, A. G, and B.Y. Chen, "An Efficient Implementation of Artificial Neural Networks with K-fold Cross-validation for Process Optimization," *J. Inf. Technol.*, vol. 20, no. 4, pp. 1213-1225, July 2019.